

# First observation of gamma-rays from the proton emitter $^{171}\text{Au}$

T. Bäck<sup>1,a</sup>, B. Cederwall<sup>1</sup>, K. Lagergren<sup>1</sup>, R. Wyss<sup>1</sup>, A. Johnson<sup>1</sup>, D. Karlgren<sup>1</sup>, P. Greenlees<sup>2</sup>, D. Jenkins<sup>3</sup>, P. Jones<sup>2</sup>, D.T. Joss<sup>4,b</sup>, R. Julin<sup>2</sup>, S. Juutinen<sup>2</sup>, A. Keenan<sup>2</sup>, H. Kettunen<sup>2</sup>, P. Kuusiniemi<sup>2</sup>, M. Leino<sup>2</sup>, A.-P. Leppänen<sup>2</sup>, M. Muikku<sup>5</sup>, P. Nieminen<sup>2</sup>, J. Pakarinen<sup>2</sup>, P. Rahkila<sup>2</sup>, and J. Uusitalo<sup>2</sup>

<sup>1</sup> Department of Physics, Royal Institute of Technology, SE-10691 Stockholm, Sweden

<sup>2</sup> Department of Physics, University of Jyväskylä, P.O. Box 35, FIN-40351, Jyväskylä, Finland

<sup>3</sup> Oliver Lodge Laboratory, Department of Physics, University of Liverpool, Liverpool, L69 7ZE, UK

<sup>4</sup> School of Chemistry and Physics, Keele University, Keele, Staffordshire, ST5 5BG, UK

<sup>5</sup> STUK - Radiation and Nuclear Safety Authority, P.O. Box 14, 00881 Helsinki, Finland

Received: 2 September 2002 /

Published online: 25 March 2003 – © Società Italiana di Fisica / Springer-Verlag 2003

Communicated by J. Äystö

**Abstract.** Gamma-rays from the alpha- and proton-unstable nuclide  $^{171}\text{Au}$  have been observed for the first time. The gamma-rays were correlated with both a proton- and an alpha-particle decay branch, confirming that the nucleus decays by alpha and proton emission from a single ( $11/2^-$ ) state. The measurement confirms the previously determined half-lives for these particle decays but the present values are of higher precision. In addition, a longer half-life than determined in previous work was measured for the proton-unstable tentative ground state. The results are discussed in relation to structures in neighbouring nuclei and compared with a Strutinsky-type TRS calculation.

**PACS.** 23.50.+z Decay by proton emission – 23.60.+e Alpha decay – 23.20.Lv Gamma transitions and level energies – 21.10.Tg Lifetimes

## 1 Introduction

The experimental frontier for neutron-deficient nuclides in the mass region around  $A \approx 170$  has been significantly advanced in recent years [1–11]. The fusion-evaporation cross-sections for the production of these nuclei are typically very small, and the experiments therefore require both effective and very selective means of detection. A majority of the nuclides in this region decay by alpha emission. The recoil-alpha tagging technique [12,13] has been of vital importance for revealing various interesting phenomena in the internal structure of these nuclei. A number of nuclides in the region have shown shape polarisation effects. These are generally associated with 2p-2h excitations (oblate shapes) or 4p-4h or higher excitations (prolate shapes) and/or the occupation of shape-driving high- $j$  intruder orbitals. The signature of such effects has been low-lying quadrupole phonon excitations of the spherical core, or shape coexistence features, where a number of low-lying bands in the same nuclide correspond to different shapes. Such phenomena are well established near the  $Z = 82$  shell closure in this mass region [1,4,7,14–17].

One important question yet to be answered is how the structure of nuclides in this region develops as we go well beyond the proton drip line, to the point where proton decay starts to compete with alpha decay. For nuclei that decay with proton emission, the same recoil-decay tagging technique as with alpha emitters can be used, but with a gate on the proton energy instead of on the alpha energy. However, due to the lower decay energies, the experimental conditions are more demanding.

The case of  $^{171}\text{Au}$  is especially interesting due to its unusual particle decay characteristics. This very neutron-deficient nuclide lies 7 neutrons outside of the proton drip line [18]. In the heavier proton-unbound gold isotopes, proton decay rates are slow to compete with alpha emission due to the difference in decay  $Q$ -values. In the case of  $^{171}\text{Au}$  however, the alpha and proton decay channels are of about equal strength. In earlier work [19,20] it was inferred from the similar measured half-lives due to alpha and proton emission, respectively, that these proceed from the same (assigned  $11/2^-$ ) state. By comparing gamma-ray spectra gated on alpha and proton energies, respectively, the decay-tagging technique can in this case be used to confirm the origin of the proton and alpha decay branches. It also gives us the rare opportunity to study the internal structure of a nucleus that emits alpha

<sup>a</sup> e-mail: back@nuclear.kth.se

<sup>b</sup> Present address: CRLC, Daresbury Laboratory, Daresbury, Warrington, WA4 4AD, UK.

particles and protons with about the same probability. Proton emission from a state in  $^{171}\text{Au}$  at lower energy than the assigned  $11/2^-$  state has also been observed [20]. From half-life considerations this state has been interpreted as being built on the  $\pi s_{1/2}$  orbital.

Recently, Kondev *et al.* [8] studied excited states in three odd-mass gold isotopes. Evidence for deformed nuclear shapes in  $^{175}\text{Au}$  and  $^{177}\text{Au}$  was found, corresponding to the occupation of the  $\pi i_{13/2}$  high- $j$  intruder orbital. The nuclide  $^{175}\text{Au}$  revealed shape coexistence features, typical for the region, with band structures seemingly corresponding to three different deformations. Interestingly, the lighter  $^{173}\text{Au}$  isotope showed no signs of collectivity.

The present data complement this picture, extending the odd-mass gold systematics of gamma-spectroscopy data to  $A = 171$ . The aim of the experiment was to investigate whether the protons and alpha particles in fact do originate from the same state, and to study the nuclear structure by observing gamma-ray emission from excited states above that state.

## 2 Experimental details

The experimental set-up consisted of the RITU [21, 22] recoil separator in conjunction with the JUROSPHERE [23] germanium detector array. A beam of enriched  $^{78}\text{Kr}$  was extracted from the 14.5 GHz ECR ion source and accelerated to 370 MeV using the K130 cyclotron at the JYFL facility in Jyväskylä, Finland. The target bombarded by the krypton ions was an isotope enriched (96.52%)  $^{96}\text{Ru}$  foil with a thickness of  $500 \mu\text{g}/\text{cm}^2$ . The centre-of-target beam energy was approximately 363 MeV.

The JUROSPHERE detectors were arranged around the target and consisted of fifteen EUROGAM-I-type [24] detectors, five TESSA-type [25] detectors, and five NORDBALL-type [26] detectors. The total photo-peak efficiency of the array was about 1.5% at 1.3 MeV. The charge and velocity focusing recoil separator RITU was filled with helium gas at a pressure of 0.6 mbar. RITU was used to separate the reaction products (with an efficiency of about 40%) from the beam particles and from the fission background. The recoils were implanted in a focal plane detector consisting of 16 silicon strips with a total area of  $80 \times 35 \text{ mm}^2$ . Each strip is position sensitive, so that the whole array has a large number of effective “pixels”. Therefore, recoil signals can be correlated with the subsequent alpha or proton decay as long as the total count rate is low in comparison to the half-life in question. The recoil signals are in turn correlated with the JUROSPHERE events, so that the prompt gamma-rays belonging to a nucleus with known particle decay energies can be extracted. This method is known as the recoil-decay tagging (RDT) [12, 13] technique. Two sets of amplifiers with different gains were connected to the silicon strip array. The high-gain amplifiers produced the alpha and proton energy spectrum. The low-gain amplifiers produced a spectrum where an energy gate could be set to discriminate the recoils from the particle decay, and from the scattered beam

hitting the focal plane detector. In order to be able to correlate the recoil events with the particle decay events, a microsecond clock was used to time stamp every event.

In order to clean the data further, we used two ancillary detector systems. First, a multi-wire proportional avalanche counter (MWPAC) in front of the silicon strip detector was used to discriminate recoils and scattered beam from the particle decay in the strip detector. In addition, the decay particles leaving only a part of their energy in the silicon detector and hitting the MWPAC could be rejected. Furthermore, a second silicon detector, behind the strip detector, was used to veto out the energetic protons and alpha particles flying through the recoil separator and punching through the strip detector. This system has been described in detail by Kettunen *et al.* [27]. These two background reduction systems are especially important when detecting protons, due to the high background level at their relatively low energy. Finally, a single germanium detector was placed behind the focal plane in order to enable detection of gamma-rays and X-rays from daughter products.

Data were collected on magnetic tapes and sorted offline.

## 3 Results

The  $^{171}\text{Au}$  recoils were detected at the RITU focal plane at a rate of approximately 1 nucleus per minute. With a beam intensity of 7 pA and a RITU efficiency of 40%, this corresponds to a cross-section close to  $0.6 \mu\text{b}$  for the  $p2n$  channel in the fusion-evaporation reaction.

The recoil-correlated alpha and proton energy spectra from the high-gain amplifiers are shown in fig. 1a. The search time following a recoil implant was limited to 8 ms. Due to the relatively short half-life of  $^{171}\text{Au}$ , the peaks corresponding to the charged-particle decay of  $^{171}\text{Au}$  are enhanced relative to a large number of much stronger channels. The peaks are also well separated from other nuclei in energy, as can be seen in the figure. At an even shorter search time of  $100 \mu\text{s}$ , the fast proton decay from the  $1/2^+$  state of  $^{171}\text{Au}$  is clearly visible, fig. 1b.

Using the microsecond clock written to every event, the half-lives of the three charged-particle decays could be extracted. For the 6996 keV alpha decay and the 1692 keV protons we obtained half-lives of  $1013(25) \mu\text{s}$  and  $1015(28) \mu\text{s}$ , respectively. For the 1444 keV protons we measured a half-life of  $37_{-5}^{+7} \mu\text{s}$ . The events used to determine the 1444 keV proton half-life were correlated with the subsequent 6.55 MeV alpha decay of  $^{170}\text{Pt}$  in order to suppress background noise. While the first two  $T_{1/2}$ -values are in agreement with earlier data ( $T_{1/2}^\alpha = 1.02(13) \text{ ms}$ ,  $T_{1/2}^p = 1.03(15) \text{ ms}$ ), the fast proton half-life is somewhat longer than previously observed ( $T_{1/2} = 17_{-5}^{+9} \mu\text{s}$ ) [19, 20]. The present values have smaller uncertainties due to better statistics.

The proton decay of  $^{171}\text{Au}$  is being studied in further detail and more information on the proton energies is soon to be published by Kettunen *et al.* [28]. The energy values

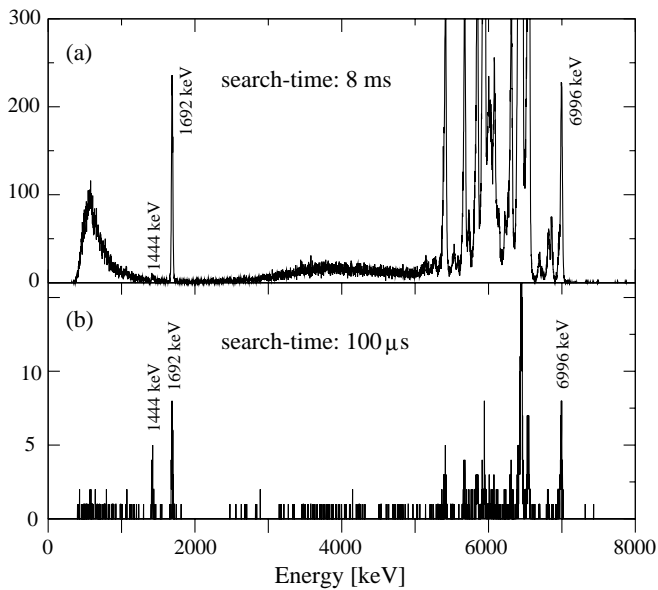


**Fig. 1.** The energy spectrum from the high-gain amplifiers connected to the focal plane silicon strips of RITU. The peaks belonging to  $^{171}\text{Au}$  are indicated by their respective energies. The peaks between 5 and 7 MeV correspond to the alpha decay from a large number of nuclides produced in the compound-nucleus reaction. The spectrum in (a) is generated using a search time of 8 ms following the recoil implants, suitable for extracting the information for the 1 ms proton and alpha decays of the  $11/2^-$  state. Panel (b) shows the same spectrum, but with a  $100\ \mu\text{s}$  search time. The 1444 keV peak from the fast proton decay from the  $1/2^+$  state is clearly visible. Gates on the 1692 keV and 6996 keV peaks were used to extract the energies of gamma-rays depopulating states above the  $11/2^-$  state. Particle energies are from Poli *et al.* [20].

for the charged particle decay of  $^{171}\text{Au}$  used in this article are all from Poli *et al.* [20].

By gating on the alpha and proton energy peaks of  $^{171}\text{Au}$  and correlating these decays to implanted recoils, and to gamma-rays detected at the target position, we could extract data on excited states in  $^{171}\text{Au}$  de-excited by gamma-ray transitions. The 1.5% photo-peak efficiency of JUROSPHERE enabled detection of 30 counts in the strongest gamma-ray peak of  $^{171}\text{Au}$ . The gamma-ray energy spectra tagged by the 6996 keV alpha line and the 1692 keV proton line are displayed in fig. 2, panels (a) and (b), respectively.

The fact that the strongest peaks are visible in both (a) and (b) indicates that both the proton and the alpha decays proceed from a single state. This confirms the earlier assumption of decay from a single  $(11/2^-)$  state [19,20]. Combining the measured half-lives of the proton and alpha branches, we obtained a half-life of  $1014(19)\ \mu\text{s}$  for this level. Panel (c) shows the sum of the alpha and proton gates, giving us the full information of the present data on the states above the  $11/2^-$  state. The fast 1444 keV proton line was unfortunately too weak to produce a useful gamma-ray spectrum.

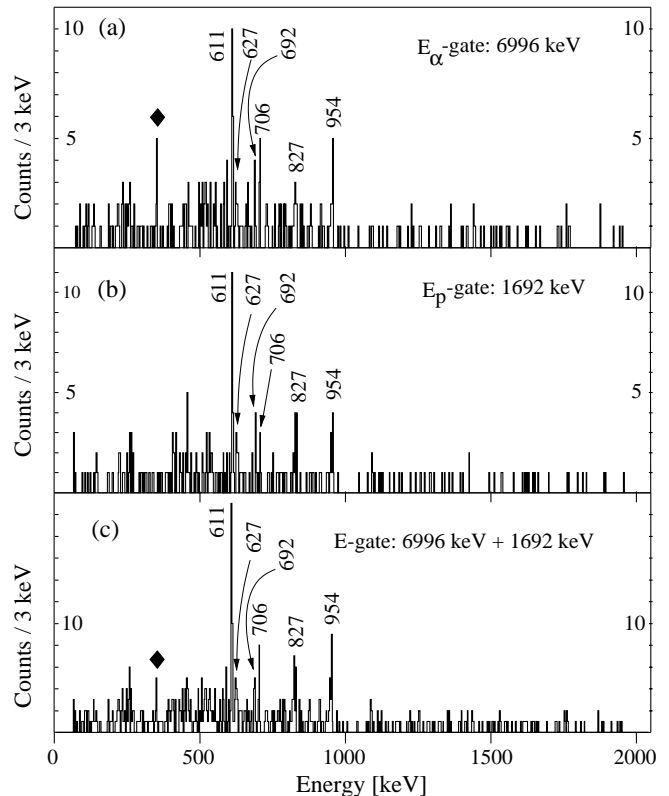


**Fig. 2.** Gamma-ray spectra from the decay of excited states in  $^{171}\text{Au}$ . The spectrum in (a) shows gamma-rays correlated with the 6996 keV alpha decay of  $^{171}\text{Au}$ . A gate on the 1692 keV proton decay line in  $^{171}\text{Au}$  generated the spectrum in (b). Adding the 6996 keV and 1692 keV events gave the spectrum in (c). All spectra are produced using a recoil/decay search time of 8 ms. The most intense peaks found in both the alpha-gated spectrum and the proton-gated spectrum are indicated with their respective energies. A peak at 352 keV (filled diamond) is seen only in the alpha-gated spectrum. The assignment of this peak to  $^{171}\text{Au}$  is therefore somewhat uncertain.

**Table 1.** Observed gamma-rays, in order of intensity in the  $\alpha + p$  spectrum, from  $^{171}\text{Au}$  in coincidence with the proton and alpha decays, respectively.

Energy (keV)	Relative intensities		
	$\alpha$	$p$	$\alpha + p$
611(3)	15(6)	15(5)	30(7)
954(5)	7(3)	7(3)	15(5)
827(5)	6(3)	7(3)	12(4)
706(5)	6(3)	2(3)	9(4)
626(6)	4(3)	5(3)	9(4)
691(8)	3(3)	4(3)	7(3)

No analysis using  $\gamma\gamma$ -coincidences was possible, due to the low statistics. This made the construction of a level scheme above the  $11/2^-$  state rather ambiguous, even though some conclusions could be drawn from the relative intensities. The observed gamma-rays are listed in table 1.

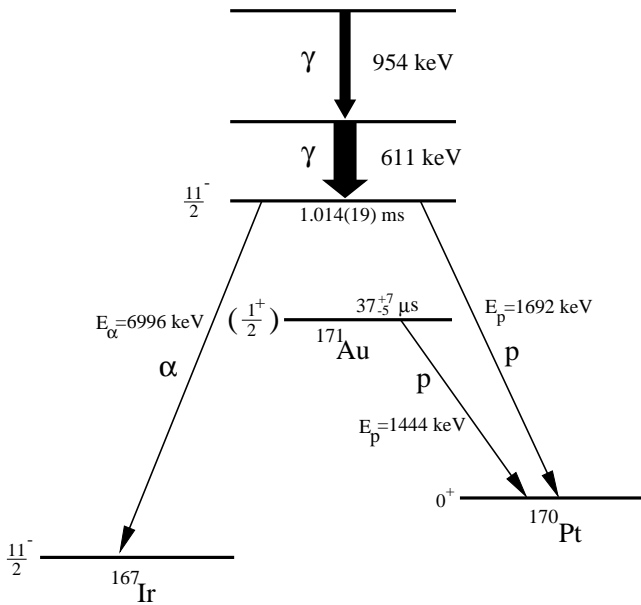


**Fig. 3.** The tentative level scheme of  $^{171}\text{Au}$ . All gamma-rays given in table 1 are seen in both the 1692 keV proton gate and the 6996 keV alpha gate, confirming that the two particle decays in fact occur from the same state. No states above the  $11/2^-$  level were known previous to the present experiment. The order of the gamma-rays feeding the  $11/2^-$  state is unknown but the two most intense gamma-ray transitions observed (611 keV and 954 keV) are tentatively assigned as a cascade feeding the  $11/2^-$  state.

## 4 Discussion

The present results complement earlier studies on light odd-mass gold isotopes with the first information on excited states in  $^{171}\text{Au}$ . Based on particle decay measurements, Davids *et al.* [19] and Poli *et al.* [20] concluded that among the available proton orbitals, the  $\pi s_{1/2}$  and  $\pi h_{11/2}$  are the most likely single-particle configurations to be responsible for the two particle-emitting states of  $^{171}\text{Au}$ , see fig. 3. Kondev *et al.* [8] showed that the isotopes  $^{175,177}\text{Au}$  feature band structures based on the  $h_{11/2}$ ,  $i_{13/2}$ , and  $h_{9/2}$  orbitals. In the heavier odd-mass gold isotopes ( $A = 179$ – $185$ ), the  $h_{9/2}$  proton orbital becomes important for describing the low-lying states [29–31].

It is difficult to make a firm interpretation of the nuclear structure of  $^{171}\text{Au}$  based on the rather limited information obtained from gamma-ray detection in the present work. However, the lack of any low-lying rotational structures is in agreement with the theoretical predictions of a near-spherical nuclear shape, see below. When comparing with the heavier odd-mass gold isotopes we see a shift in deformation from the rotational structures of  $^{177}\text{Au}$  and  $^{175}\text{Au}$  to the irregular level pattern of  $^{173}\text{Au}$  [8]. The present data of  $^{171}\text{Au}$  complement this picture. The two most intense gamma-rays in  $^{171}\text{Au}$  (611 keV, 954 keV) show a striking resemblance to the structure above the  $11/2^-$  state in  $^{173}\text{Au}$  (592 keV, 970 keV) [8]. There is no sign of any rotational structures like the bands that dominate the spectra of  $^{177}\text{Au}$  and  $^{175}\text{Au}$ . This change in

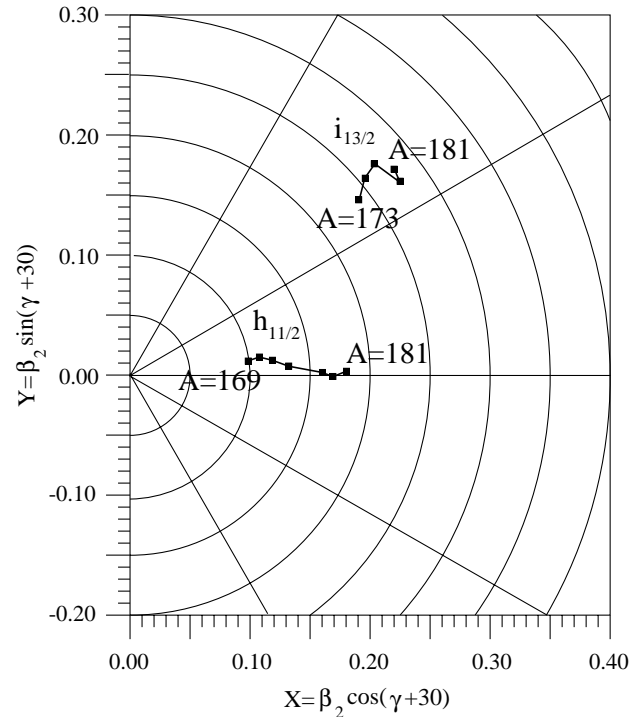


**Fig. 4.** The deformation of the light odd-mass gold isotopes for two different configurations. The minimum corresponding to the  $\pi i_{13/2}$  orbital is calculated at  $\hbar\omega = 0.16$  MeV, and the  $\pi h_{11/2}$  minimum at  $\omega = 0$ . The  $\pi h_{11/2}$  deformation decreases as we go towards the lightest isotopes, reaching a value close to  $\beta_2 = 0.1$  at  $^{171}\text{Au}$ . The  $\pi i_{13/2}$  minimum, on the other hand, is stabilised at a much larger deformation of  $\beta_2 \approx 0.25$ . This minimum becomes quite energy-unfavoured below  $A = 175$ .

structure can be interpreted in terms of the energy difference between configurations corresponding to the  $h_{11/2}$  and  $i_{13/2}$  proton orbitals. The earlier conclusions [19,20] made about the shape of  $^{171}\text{Au}$ , where a proton in the  $h_{11/2}$  orbital is coupled to the near-spherical core of  $^{170}\text{Pt}$ , therefore seem to be confirmed by the present data.

To illustrate this from a theoretical point of view, we have used a Strutinsky-type calculation based on a Woods-Saxon potential. The applied model [32] treats pairing interactions self-consistently, and uses the Lipkin-Nogami approach [33,34] to project approximate particle numbers. The energy can be minimised in the rotating frame of reference with respect to the  $\beta_2$ ,  $\beta_4$ , and  $\gamma$  deformation parameters. Total Routhian surfaces (TRS) can also be extracted from the energy mesh in order to visualise energy minima. In fig. 4 we have plotted the predicted deformation parameters  $(\beta_2, \gamma)$  for a number of gold isotopes. Energy minima in the TRS corresponding to the  $h_{11/2}$  and  $i_{13/2}$  orbitals are indicated. The  $h_{11/2}$  minimum approaches a spherical shape as we enter the proton-unstable region, reaching a  $\beta_2$  deformation close to 0.1 ( $\gamma \approx -25^\circ$ ) at  $^{171}\text{Au}$ . In contrast, the  $i_{13/2}$  minimum stays rather constant at a larger deformation ( $\beta_2 \approx 0.25$ ) near the prolate axis. The positions of both minima are rather insensitive to the rotational frequency. Because of this, the  $i_{13/2}$

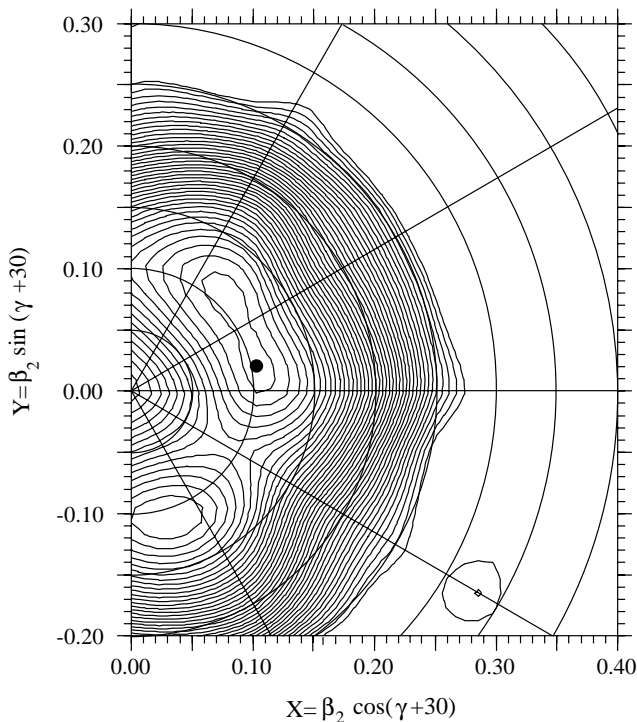


**Fig. 5.** A total Routhian surface for  $^{171}\text{Au}$ , calculated for the negative-parity configuration at zero rotational frequency. The same nuclear shape generates three energy minima at  $\beta_2 \approx 0.1$  but at different  $\gamma$ -values due to the symmetries at  $\omega = 0$ . The minimum used to make the  $h_{11/2}$  plot in fig. 4 is indicated by a filled circle.

minimum position is plotted at  $\hbar\omega = 0.16$  MeV, where the minimum is deep enough to be traced over a larger number of nuclei. The TRS for the negative-parity configuration at zero rotational frequency is plotted in fig. 5. The minima correspond to the  $h_{11/2}$  proton orbital configuration. Due to symmetries at  $\omega = 0$  the minimum is seen in three locations. The minimum chosen in fig. 4 is marked with a filled circle. Kondev *et al.* [8] showed that the excitation energy of the  $i_{13/2}$  band members increases quickly relative to the  $h_{11/2}$  states as the neutron number decreases for the lightest gold isotopes. Our calculation gave the same result, explaining why our data show no indication of a rotational structure corresponding to a deformed  $i_{13/2}$  configuration.

The half-lives for the alpha and proton decays from the assigned  $11/2^-$  state are in the present work measured with higher precision than before. The obtained  $T_{1/2}$  values are in agreement with earlier observations. On the other hand, the measured half-life for the fast proton decay is somewhat longer than previously observed. As discussed by Poli *et al.* [20], this value determines the choice between a  $\pi s_{1/2}$  and a  $\pi d_{3/2}$  configuration for the ground state of  $^{171}\text{Au}$ . The proton emission half-life for the  $\pi s_{1/2}$  configuration was predicted by Poli *et al.* to 20  $\mu\text{s}$ , using a spectroscopic factor of 0.22. The present half-life value of  $37_{-5}^{+7} \mu\text{s}$  may suggest a different interpretation, possibly involving a  $\pi d_{3/2}$  admixture. When calculating the occupation factors of protons in the two lowest states above the

Fermi level of  $^{170}\text{Pt}$  we obtained a value of  $v^2 = 0.50$  (0.16) for the state dominated by  $d_{3/2}$  ( $s_{1/2}$ ). Note that, according to our calculations, these states were rather mixed.

## 5 Summary

In summary, we have for the first time identified gamma-rays emitted from the very neutron-deficient nucleus  $^{171}\text{Au}$ . The data confirms the assignment of proton and alpha decays from a single ( $11/2^-$ ) state. The lack of any rotational structure in the gamma spectrum is in agreement with the previous assumption of a near spherically shaped nucleus. The half-lives of the alpha and proton decays from the  $11/2^-$  state, as well as the proton decay half-life for the  $1/2^+$  state have also been measured with higher precision than before.

The authors would like to thank Geirr Sletten and Jette Sørensen at NBI, Denmark, for preparing the targets and Sean Freeman at Manchester University, UK, for providing the  $^{96}\text{Ru}$  material. We also thank Robert Page at Liverpool University, UK, for the use of the  $^{78}\text{Kr}$  gas. This work has been supported by the Academy of Finland under the Finnish Centre of Excellence Programme 2000-2005 (Project No. 44875, Nuclear and Condensed Matter Physics Programme at JYFL). We also acknowledge the financial support from the Swedish Research Council and the European Community, *Access to Research Infrastructure action of the Improving Human Potential Programme* (Contract No. HPRI-CT-1999-00044).

## References

1. B. Cederwall *et al.*, Phys. Lett. B **443**, 69 (1998).
2. S.L. King *et al.*, Phys. Lett. B **443**, 82 (1998).
3. R.A. Bark *et al.*, Nucl. Phys. A **646**, 399 (1999).
4. R.A. Bark *et al.*, Nucl. Phys. A **657**, 113 (1999).
5. S.L. King *et al.*, Phys. Rev. C **62**, 067301 (2000).
6. D.T. Joss *et al.*, Nucl. Phys. A **689**, 631 (2001).
7. R. Julin *et al.*, J. Phys. G **27**, R109 (2001).
8. F.G. Kondev *et al.*, Phys. Lett. B **512**, 268 (2001).
9. F.G. Kondev *et al.*, Nucl. Phys. A **682**, 487c (2001).
10. M.B. Smith *et al.*, Nucl. Phys. A **682**, 433c (2001).
11. D.E. Appelbe *et al.*, Phys. Rev. C **66**, 014309 (2002).
12. E.S. Paul *et al.*, Phys. Rev. C **51**, 78 (1995).
13. R.S. Simon *et al.*, Z. Phys. A **325**, 197 (1986).
14. K. Helariutta *et al.*, Acta Phys. Pol. B **30**, 1267 (1999).
15. F.G. Kondev *et al.*, Phys. Rev. C **61**, 011303(R) (2000).
16. F.G. Kondev *et al.*, Phys. Rev. C **62**, 044305 (2000).
17. F.G. Kondev *et al.*, Phys. Lett. B **528**, 221 (2002).
18. G. Audi, A.H. Wapstra, Nucl. Phys. A **595**, 409 (1995).
19. C.N. Davids *et al.*, Phys. Rev. C **55**, 2255 (1997).
20. G.L. Poli *et al.*, Phys. Rev. C **59**, 2979 (1999), Rapid Communication.
21. M. Leino *et al.*, Nucl. Instrum. Methods B **99**, 653 (1995).
22. M. Leino, Nucl. Instrum. Methods B **126**, 320 (1997).
23. R. Julin *et al.*, Acta Phys. Pol. B **32**, 645 (2001).
24. C.W. Beausang *et al.*, Nucl. Instrum. Methods A **313**, 37 (1992).

25. P.J. Nolan *et al.*, Nucl. Instrum. Methods A **236**, 95 (1985).
26. G. Sletten, in *International Seminar on the Frontier of Nuclear Spectroscopy*, edited by Y. Yoshishawa. (World Scientific, Singapore, 1993).
27. H. Kettunen *et al.*, Acta Phys. Pol. B **32**, 989 (2001).
28. H. Kettunen *et al.*, in preparation
29. A.J. Larabee *et al.*, Phys. Lett. B **169**, 21 (1986).
30. W.F. Mueller *et al.*, Phys. Rev. C **59**, 2009 (1999).
31. W.F. Mueller *et al.*, in preparation.
32. W. Satuła, R. Wyss, Phys. Scr. T **56**, 159 (1995).
33. H.C. Pradhan, Y. Nogami, J. Law, Nucl. Phys. A **201**, 357 (1973).
34. W. Satuła *et al.*, Nucl. Phys. A **578**, 46 (1994).